ISTITUTO NAZIONALE DI FISICA NUCLEARE

Sezione di Milano

INFN/TC–99/25
3 Novembre 1999

DEVELOPMENT AND CHARACTERIZATION OF ITD MULTIFILAMENTARY NB_3SN SUPERCONDUCTORS FOR 10–15 T FIELD MAGNETS

M. Pojer, L. Rossi

Dipartimento di Fisica dell'Università degli Studi di Milano, INFN–Sezione di Milano
Laboratorio LASA, Via Fratelli Cervi 201, I–20090 Segrate (MI), Italy

Abstract

Inside the European project LHC (the Large Hadron Collider which is currently under construction at CERN), the LASA lab of INFN–Milan has recently carried out a feasibility study and a design of a Nb_3Sn low–β quadrupole as a possible future candidate for the inner triplet in the Interaction Region of LHC. A preliminary research on material has been developed, centered on ITD (Internal Tin Diffusion) Nb_3Sn wires characterization.

Measurements on transport properties have shown values of critical current densities as high as 1480 A/mm^2 at 12T, 4.2K, corresponding to 1860 A/mm^2 at 12T, 2.2K. I_c degradation due to cabling has also shown values contained below 15% while the degradation in condition of transversal pressure up to 200 MPa has been found to be in the range of 7% (only 1% irreversible).

One of the most important features of Nb_3Sn is its volume increase during superconducting phase formation; for this reason volume variations have been determined experimentally.

However the actual limit of these conductors is the very high value of effective filament size, as drawn out by magnetization measurements. A possible way of limiting the filament size is proposed.

A scaling law for our conductors is also proposed, with J_c as a function of magnetic field, temperature and strain.

Eventually the excellent J_c results recently obtained on a new wire are presented (J_c near 2000 A/mm^2 at 12T and 4.2K).

PACS: 85.25

Published by ***SIS–Pubblicazioni***
Laboratori Nazionali di Frascati

1. INTRODUCTION

In the context of a collaboration between CERN and INFN on LHC superconducting magnets, our lab has promoted the construction of Nb_3Sn quadrupoles with a very high field for a future upgrade of the low–beta inner triplet in the Interaction Region. Since low–beta quadrupoles control beam focalization in the interaction points, it is clear that a gain in terms of the intensity of focalization and/or coil aperture can greatly enhance machine throughputs, besides allowing the relaxation of some critical parameters. The actual project (1) has planned the construction of NbTi quadrupoles with a gradient of 220 T/m in a 70 mm aperture. NbTi technology has yet come to its ultimate practical operating level, besides which only NbSn performances can result in an effective increase in the gradient. In particular, the study of these second generation quadrupoles has led to the development of two different configurations (2): 250 T/m with a coil aperture of 85 mm and 300 T/m in a 70 mm aperture. The latter very high gradient of 300 T/m demands a non-copper current density above 1800 A/mm^2 at 12 T, the winding peak field. Other requirements are equally very important: the effective filament size must be small (10–20 μm) to minimize field distortions, cabling in Rutherford cable must result in a reduced I_c degradation and the cable itself should withstand a transverse pressure around 150 MPa in the magnet without severe I_c degradation.

Our choice for the conductor has been that of using Nb_3Sn wires produced with the internal diffusion of tin by the Italian factory Europa Metalli in the conviction of being able to obtain very high critical current density values; internal tin diffusion conductors require nevertheless precise thermal treatments and careful manipulation, due to their compound nature and brittleness.

2. INTERNAL TIN DIFFUSION NB_3SN WIRES

Europa Metalli is the first in Europe to use extensively the technique of producing Nb_3Sn by the internal diffusion of tin; this technique requires a difficult manufacturing process because of the difference in ductility between the single materials and of the low melting temperature of tin, which prevents from using thermal treatment of annealing.

ITD wires are made of a copper matrix which incorporates thousands of niobium filaments and several tens of tin filaments, reduced to dimensions of some microns by the mechanical treatment of extrusion and different cold drawings. The two layouts developed (3–Sectors and High Field, shown in figures) are substantially identical, with the Nb–1%Ti filaments arranged in 37 bundles, each one protected by an individual Nb barrier, with the Sn core at the center of the island. Differently from High Field configuration, in 3–Sectors structure the space between the filaments should favor Sn diffusion toward the periphery of the island, thus increasing homogeneity of the wire. High Field wires (in which Nb filaments are arranged around the core without empty channels), vice versa, should guarantee higher I_c values, due to the larger Nb total cross section, in spite of a retarded diffusion of tin towards outer filaments.

The content of copper is about 50%, with a Cu to non–Cu ratio which varies from 1 to 1.1 in a wire diameter of 0.8–0.9 mm.

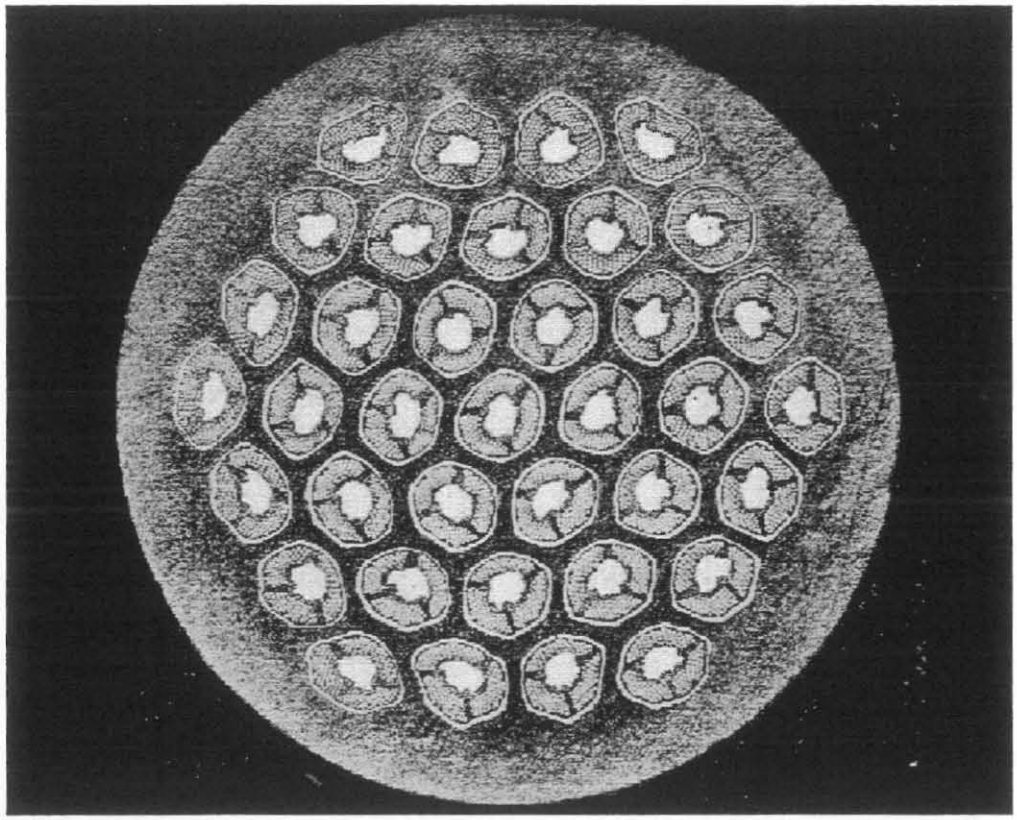

FIG. 1 - Photomicrograph of the transversal section of a 3 Sectors Nb_3Sn wire with 37 bundles; $\phi = 0.820$ mm, $\alpha = 1.1$.

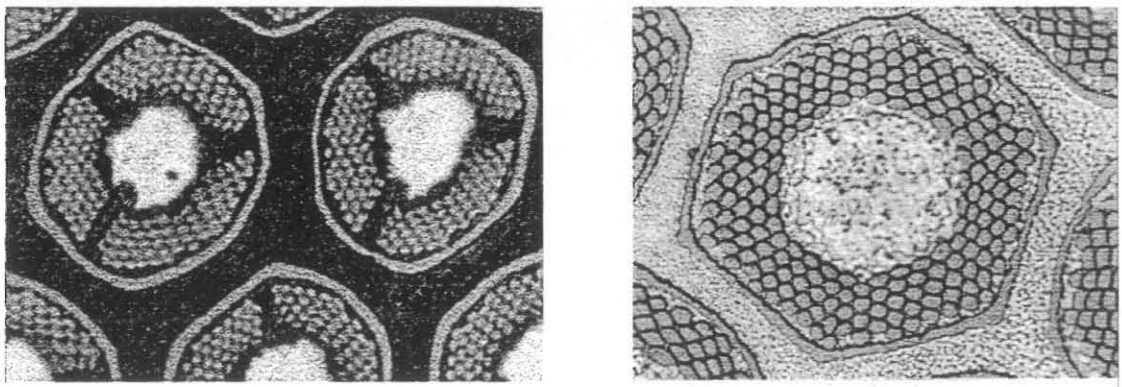

FIG. 2 - Particulars of the two layouts in which the unequal structures of the two islands are visible. (Difference in color is due to different optical vision systems)

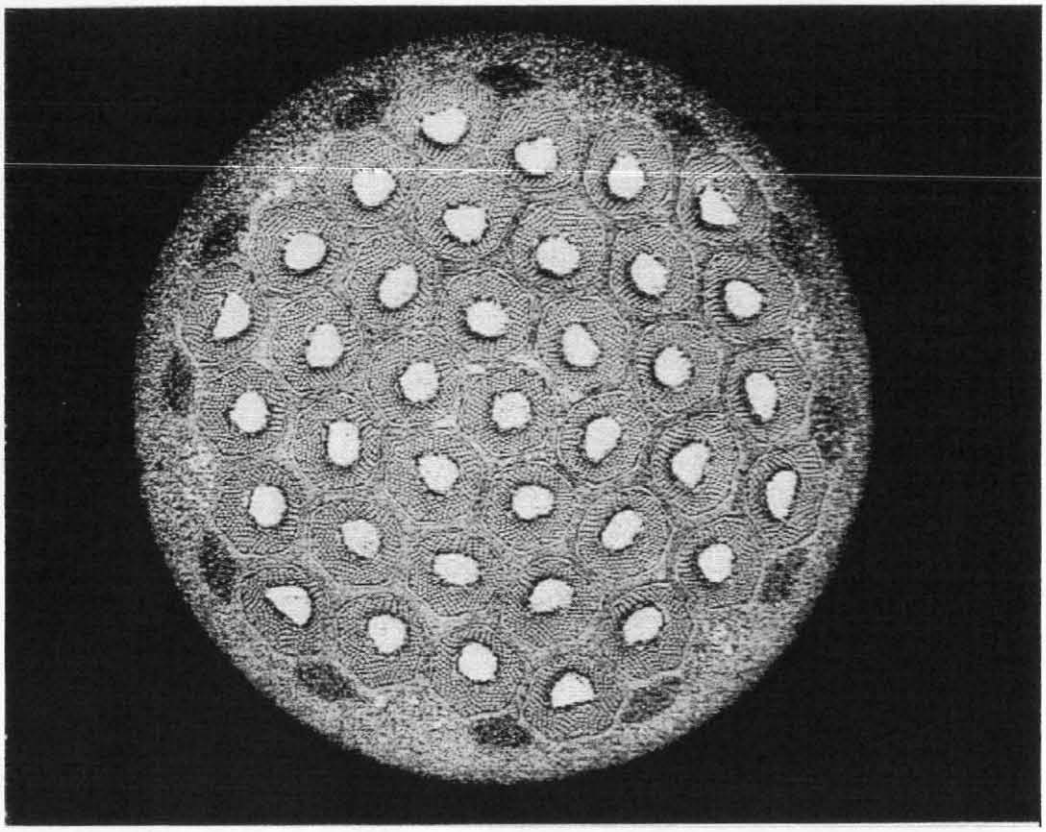

FIG. 3 - High Field layout: there are still 37 bundles but filaments are uniformly distributed around tin cores. $\phi = 0.820$ mm, $\alpha = 1.1$.

A thermal treatment of reaction is necessary to operate a solid state diffusion of tin inside niobium; it is quite complex and long:

- 175 hours @ 220 °C (± 3 °C) to produce a Cu–Sn inter–diffusion;
- 96 hours @ 340 °C (± 5 °C) to homogenize bronze;
- 180 hours @ 650 °C (± 5 °C) for solid state diffusion and superconducting layer growth.

It's important in the first step not to exceed 225 °C to avoid an excessive increase in tin volume and, above all, the formation of liquid, which could leave microscopic holes in the material when cooled (Kirkendal holes). For the same reason, the ramps of growing of temperature are quite slow (30 °C/h).

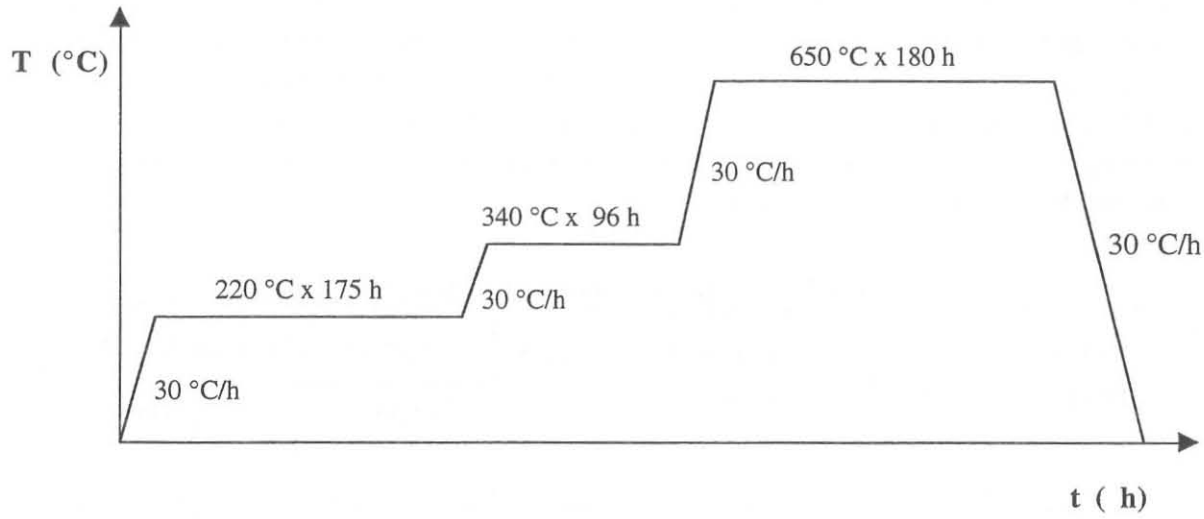

FIG. 4 – Not–scaled thermal treatment scheme.

Besides, thermal treatment must be done in vacuum or argon to avoid the formation of oxides or the absorption of impurities. Wires must finally be treated in the same form in which they will be measured (Wind & React technique) because of their brittleness after reaction.

The good results obtained in terms of critical current density are partially due to our improvement of thermal treatment.

Variations to the standard thermal scheme have also been studied, in particular the shortening or extension of the last period, which implies a different amount of superconducting material being formed.

3. VOLUME INCREASE

One important peculiarity of NbSn is its volume increase during thermal treatment, due to the formation of the superconducting phase; though negligible in short samples, it may become very important for windings where coils are mechanically contained. For this reason volume variations on single wires and cables stack have been studied, in different positions and stress conditions. The results of our measurements are summarized in Table 1.

As can be seen, for free single wires (for example, a single strand inside a drilled cylinder of ceramics, which doesn't undergo any kind of stress) there is a decrease in the length, probably due to the thermal treatment induced release of the tension accumulated during cold drawing; the same behavior is visible for free cables, where the effects of wire drawing and cabling tension add together.

Diameters of reacted wires were found to be larger than unreacted ones and the analysis of A.C.M. samples (those with different thermal treatments) demonstrates, as predictable, that the

extension of time of superconducting phase formation produces an analogue increase in volume. That is to say that thermal treatment is responsible for a new setting in which atoms are widely spaced together. Besides, it can be noted that for wires of the same kind with different diameters, the percent volume increase is higher for conductors with larger diameter (see samples *HF'96–virgin* and *HF'98–virgin* for which thermal treatment is identical). This means that, enlarging wires, tin diffusion is favored by larger spaces between Nb filaments (this is also confirmed by J_c results, as shown later).

TABLE 1 – Volume variations in thermal treatment.

CONDUCTOR IDENTIFICATION	ϕ_{strand} or cable size (mm)	POSITION	PERCENTAGE VARIATION		
			Length	Width	Thickness
3 Sectors '95 – virgin strand	0.820	free	- 0.31	-	1.8
H.F. '96 – virgin strand	0.820	free	-	-	1.8
H.F. '98 – virgin strand	0.900	free	-	-	2.2
A.C.M. 1 – virgin strand	0.900	free	-	-	2.3
A.C.M. 3 – virgin strand	0.900	free	-	-	2.4
A.C.M. 5 – virgin strand	0.900	free	-	-	3.1
KEY. - 3 Sectors '95 – cable	15.05 X 1.52 /1.3	free	-	1.8	1.5 / 1.3
FLAT - 3 Sectors '95 – cable	15.11 X 1.45	groove	- 0.35	1.7	1.4
FLAT - 3 Sectors '95 – cable	15.11 X 1.45	box	- 0.31	1.7	1.2
FLAT - 3 Sectors '95 – cable	15.11 X 1.45	U-shape	0.53	-	-

In order to give an account of the behavior of cables in a real winding of accelerator magnets, a special equipment was made as to keep the material under moderate pressure or preventing it from recovering tensions. The first one was a stainless steel plate where a groove is machined. In the groove a cable is positioned and kept under pressure by a stainless steel cap blocked by screws: the cable is free of shortening but is kept pressed inside the groove approximately as it would be in a real winding. In real coils for accelerator magnets, a stack of cables, rather than a single one, is instead kept under pressure during reaction. Also there is a need to keep under control the actual pressure value during the high temperature heat treatment. To this aim we built a stainless steel box (see fig. 5) to accommodate a stack of ten cables and to control the pressure onto the stack by special cup springs. Pressure values used while measuring are 1.2 Mpa, reducing at nearly 0.5 MPa during thermal treatment. Results obtained with groove

and box are nearly the same: length is reduced by about 0.3% (as just explained) and a thickness increase is still visible, but is now less than for single wire due to the presence of free spaces between strands.

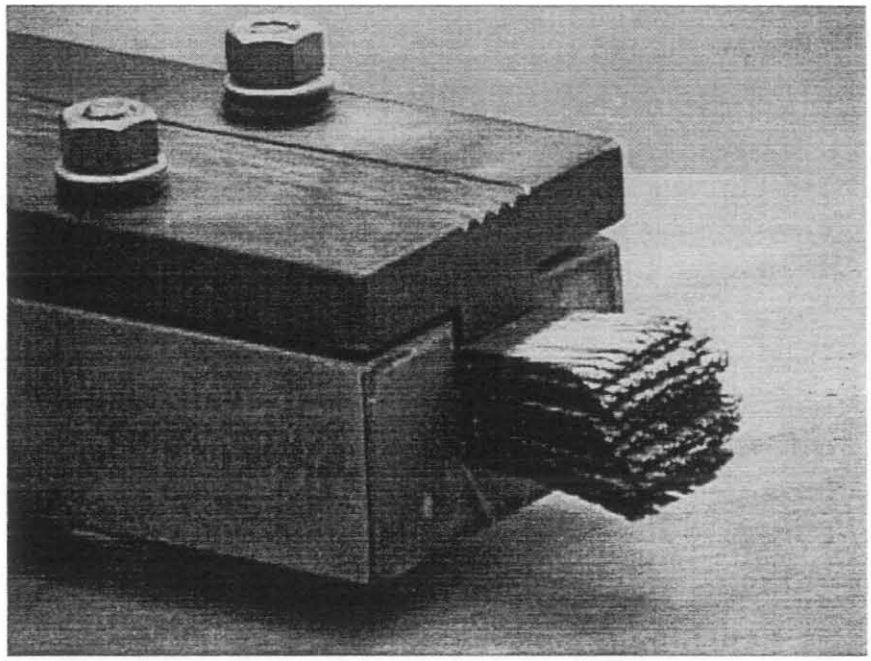

FIG. 5 – Box for volume variations measurements with a stack of ten cables.

The combination of all measurements leads to a volume increase around 3%, surely important for any type of winding and which should be so taken into account in magnet design.

Another interesting consideration is that relative to the permanent increase of length due to reaction of a cable wound onto a mandrel: one turn of cable was wound on a stainless steel half mandrel (see below), about 200 mm long, with a tensile force of 350 N, a typical value for winding in dipoles and quadrupoles; the cable is then locked against the mandrel (to simulate the other half turn) and reacted. After reaction a gap appears between mandrel and the cable at the curvature end, due to the smaller thermal contraction of Nb_3Sn/bronze/copper composite with respect to the thermal contraction of stainless steel. The gap was of the order of 1 mm over a length of 200 mm or 0.5% permanent elongation.

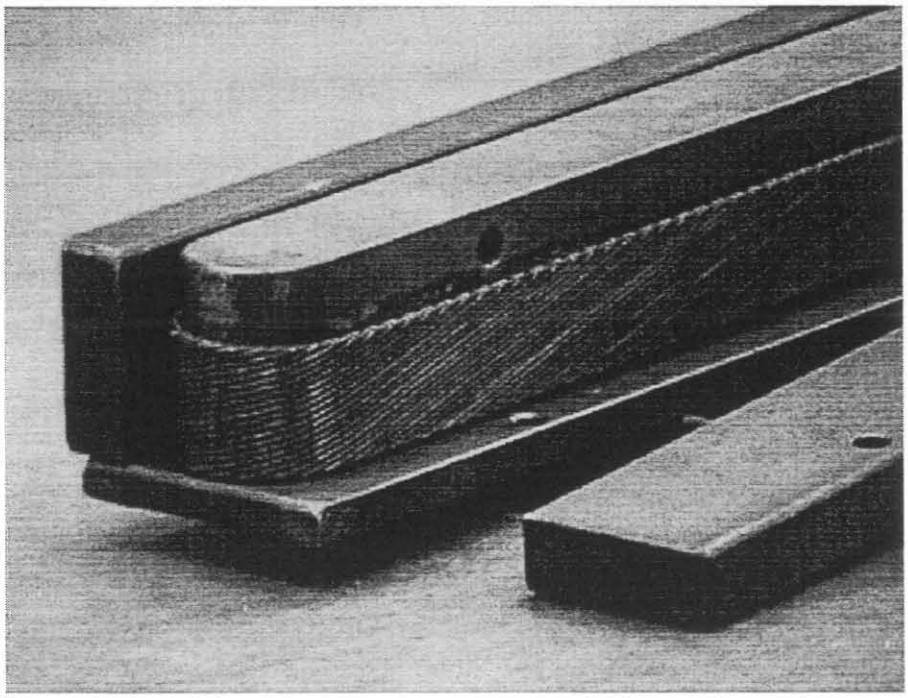

FIG. 6 – Half mandrel simulating a winding.

4. CRITICAL CURRENT

Magnetic fields necessary to make measurements of critical current densities with relatively little currents supplied are obtained with a superconducting solenoid, capable of generating in the cold bore of 53 mm magnetic fields up to 14 T at the temperature of boiling liquid helium and 15.5 T at 2.2 K (our lab is the only one in Italy to make routinely high power measurements at the super–fluid helium temperature). Super–fluid helium is obtained with a system named lambda-plate refrigerator, which is composed by a copper serpentine placed just above the magnet and in thermal contact with its helium bath. This serpentine absorbs liquid from the upper volume (always at 4.2 K) regulated by a pin valve and connected at the outside with a pump; calibrating helium flux in the serpentine and pumping away helium gas inside it down to pressures of few mbars the under-cooling of helium is obtained. In about two hours and with a pump of 40 m^3/h, the temperature inside the serpentine and so around the magnet and the sample is lowered to 2.15–2.2 K. Temperature is monitored by means of two Rh–Fe resistive probes.

Several sample holders are used for critical current measurements, but one in particular was designed and realized at LASA for NbSn, which allows current supplies up to 2000 A (see fig. 7). The experimental procedure is a 4–wires measurement. The strand, virgin or extracted from cable, is mounted in a ten turns spiral shape (as it is reacted) onto a G10, 30 mm Ø cylinder with copper ends serving as current junctions. Electrical contact and locking of wires is achieved by soldering sample ends to copper blocks for a length of about two turns. This is not a warranty of good electrical contact and may result in the appearance of resistive besides thermal disturbances; for this reason soldering takes at least two turns and voltage taps are about 30 cm long, away from the junction points. Several other taps are positioned at every junction to control potential drops along sample holder and especially protect the sample from prolonged quenches; in fact, when tension and time thresholds of 25 mV and 30 ms are exceeded, the circuit of protection, QDS (Quench Detection System), stops current.

Sample temperature during measurements is monitored by a carbon glass resistor (CGR) which is precise at almost few mK near liquid helium temperature.

We use two different power suppliers to feed the sample: the first one is made by a series of battery and can deliver continuous currents up to 2000 A at a maximum voltage of 4 V; the second one can support currents of a maximum of 10000 A, limited at 6 V, with a very low noise thanks to a DCCT controller.

Data acquisition is obtained with a HP 3852A multimeter and with a KEITHLEY 182 SDV nanovoltmeter for sample voltage, automatically recorded by means of PC interface.

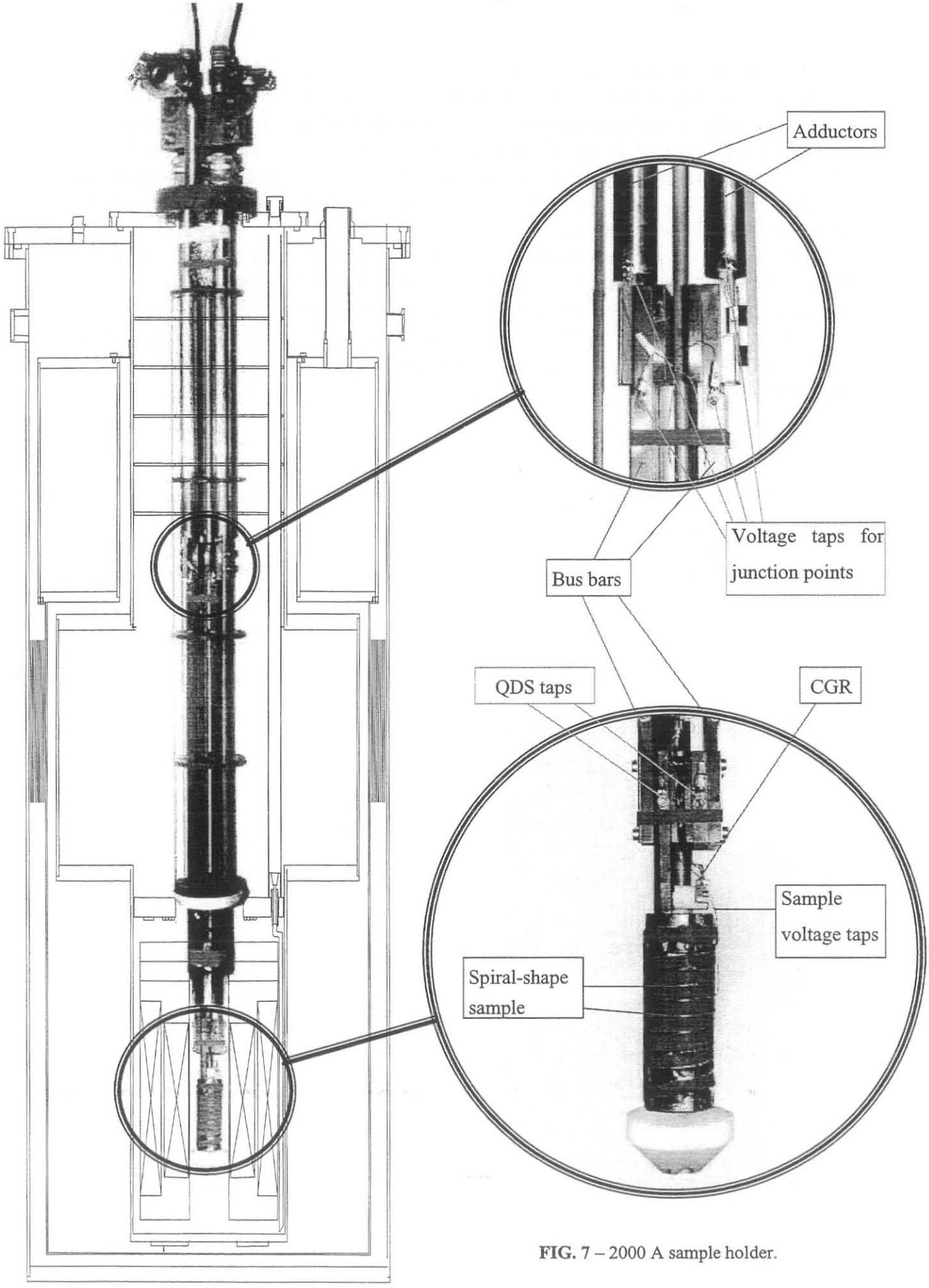

FIG. 7 – 2000 A sample holder.

The critical current I_c is determined with the electric field criterion of 10 μV/m and the critical current density is the ratio of I_c and the non-copper cross section of the wire. Due to its spiral shape, wire is not perfectly perpendicular to the applied magnetic field thus resulting in an error in the evaluation of B applied on it which is proportional to the angle between the directions of wire and magnetic field itself. This angle is nevertheless around 6°, that implies an error in magnetic field which is only 0.5–0.6%. The perpendicular orientation corresponds to the worst case (lowest J_c) but it's the relevant orientation for magnets.

The results of J_c are self–field corrected and plotted as a function of B for *EM–3Sectors–95– virgin 1* in fig.8, in the two self–field polarizations. Values are very high, especially when referred to those obtained in samples made with bronze route: 1480 A/mm^2 at 12 T, 4.2 K, and 1860 A/mm^2 at 12 T, 2.2 K. [Measurements on bronze route manufactured *VAC–Ta–I–HP–96–virgin* wire produced from Vacuumschmelze showed J_c values as "low" as 700 A/mm^2 at 12 T, 4.2 K][1].

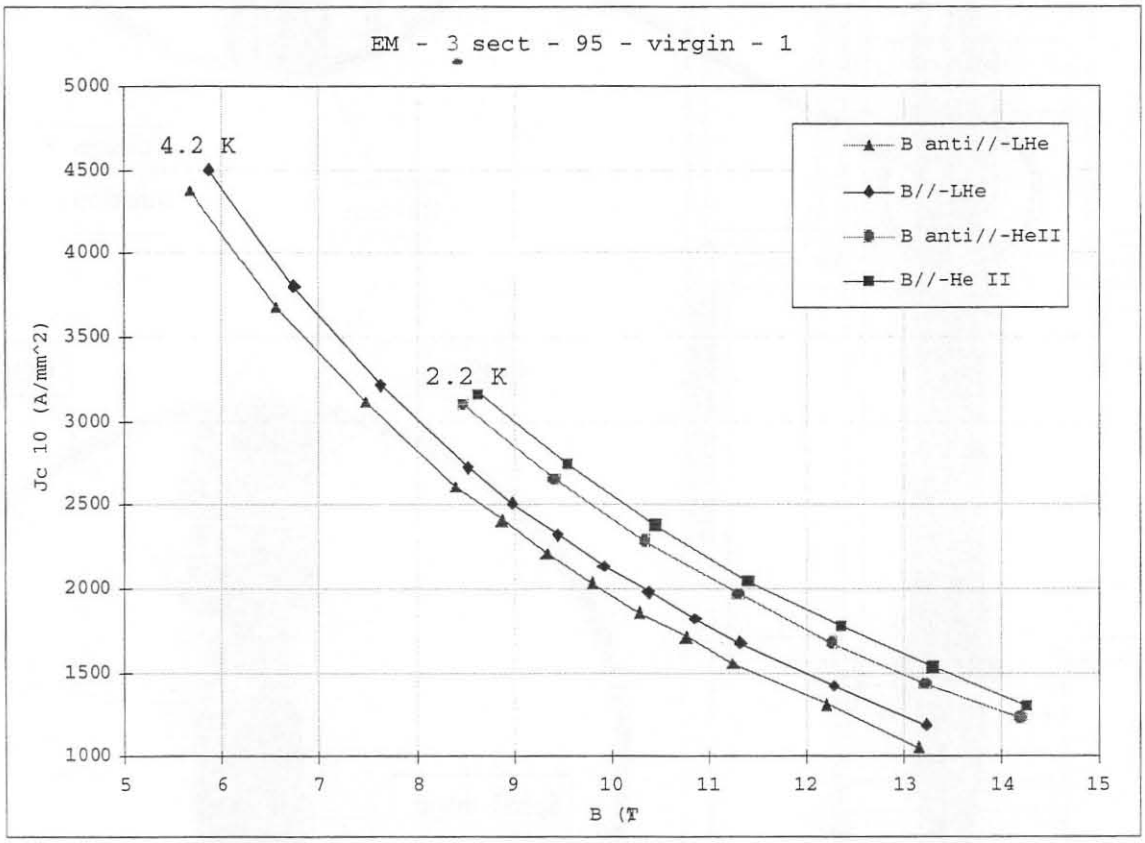

FIG. 8 – Critical current density versus magnetic field for a 3 Sectors wire at two different temperatures, 4.2 and 2.2 K, and for both field orientations (see text for details).

[1] This wire has been studied only on three samples and maybe can give better performance. However the best result obtained by the company is about 900 A/mm^2.

The shift of the data at 12 T when temperature is reduced from 4.2 K down to 2.2 K is about 1.4 T for both layouts, while the difference in critical current density from parallel to anti parallel disposition is 110 A/mm^2 in 3–Sectors wires and 60 A/mm^2 in High Field ones.

The n–value (transition index) is very good, about 40 ± 5, for 3–Sectors and less satisfactory for HF material where it ranges from 20 to 25 (see figure 9). This is explainable according to what we said about the favoring of tin diffusion by the three bronze channels in 3Sectors layout, which enhances the homogeneity with the external filaments being equally well reacted.

From the analysis of a measurement with an average noise level it was also possible to evaluate the percentage error due to the instrumentation or to the experimenter inaccuracy: I_c values are subjected to an error of 1–1.5%, while for n-value the error is higher (5-10%) because it is strongly affected by noise. Very noisy measurements and/or few points of interpolation can result in a more marked imprecision.

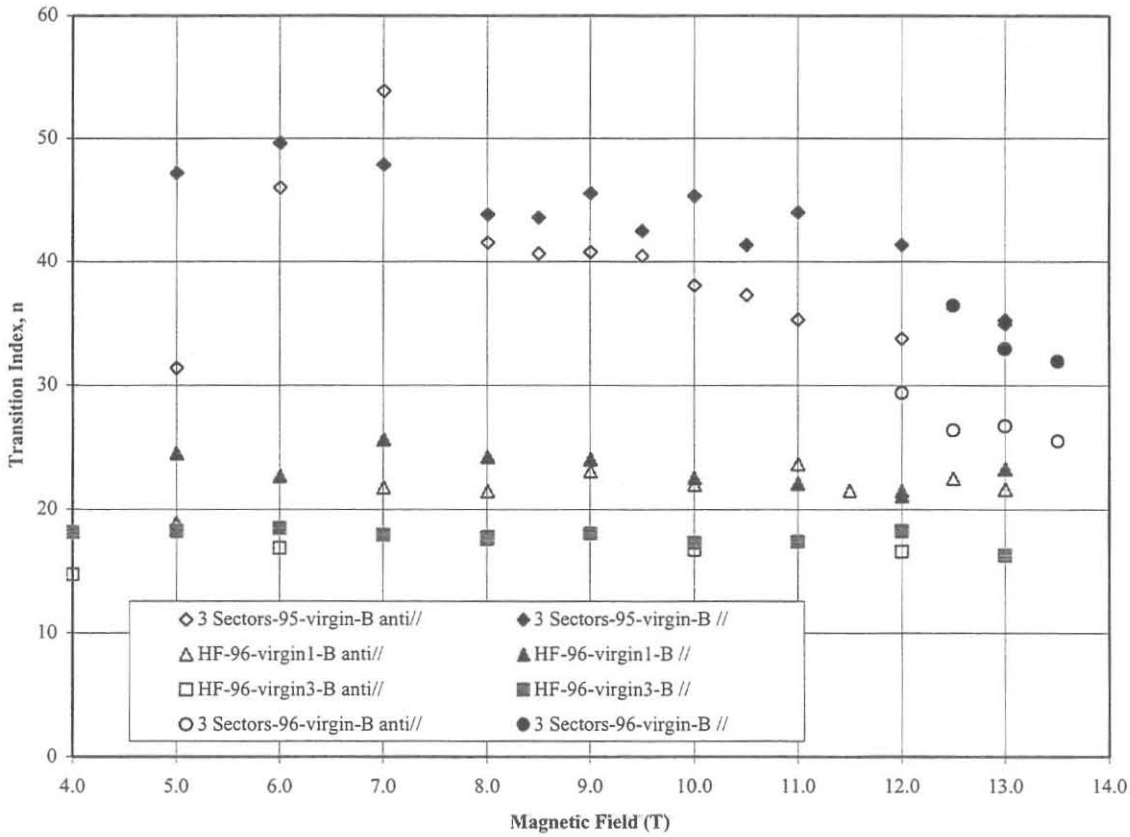

FIG. 9 – Transition index Vs magnetic field for several samples

4.1 Self-field correction

Since a current flowing in a wire always produces a magnetic field in the surroundings (self-field, B_{sf}), it is clear that critical current measurements are performed in a magnetic field which is different from bare external magnetic field and equal to the sum of this one plus sample self-field.

If we consider the wire on sample holder as a solenoid with *n* loops and approximate it for simplicity to a series of *n* planar loops, we can compute self-field generated on a loop by all other ones. Such a count was done with a numerical program for the central loop (for which the intensity of magnetic field is higher) and it was found that in the axial direction (perpendicular to each loop) the field values are 0.000756 T/A near the center of the solenoid and 0.000586 T/A far away. With the convention that self-field is said to be parallel to the external field B_{ext} when so is the field inside the solenoid (sample), we thus have that: when B_{sf} is parallel (//) to B_{ext}, maximum total field is equal to B_{ext} plus $\Delta B=I_c \cdot 0.000756$; when B_{sf} is anti-parallel (anti//) $B_{tot}=B_e+I_c \cdot 0.000586$.

4.2 Influence of thermal treatments on I_c

We have already underlined how much important is the last part of thermal treatment in the formation of Nb_3Sn, at 650 °C with diffusion of tin inside niobium. During this reaction, there are two competing processes which take place in the material:

- the section of Nb_3Sn grows continually, thus increasing I_c values;
- growth of grains inside the superconductor tends to lower the current density by the decreasing of pinning centers density (grain boundaries are in fact the privileged point of pinning of fluxoids).

What is visible is thus an increasing in critical current up to a maximum point, besides which the lessening of pinning points becomes predominant.

Variations to thermal treatment have been studied to verify this and so optimizing reaction procedure, modifying tin diffusion time, according to:

- 175 h @ 220 °C;
- 96 h @ 340 °C;
- 60 – 90 – 120 – 150 – 180 h @ 650 °C.

The resulting behavior (see fig. 11) is as expected.

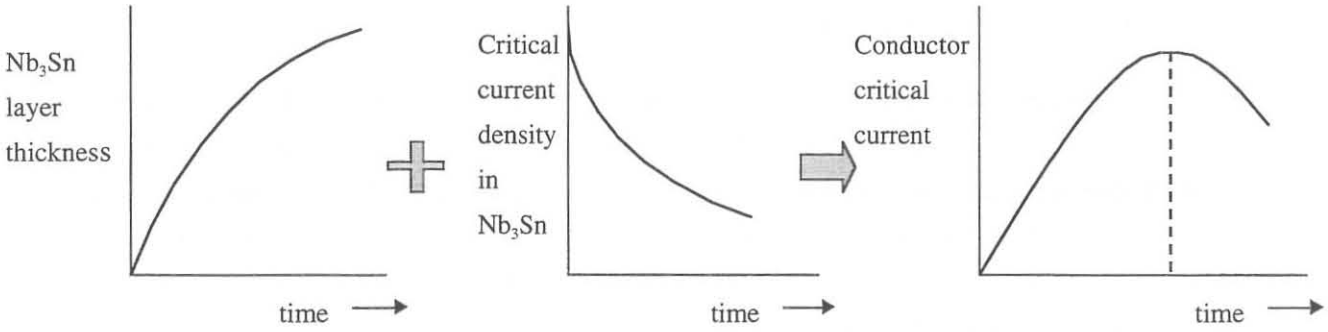

FIG. 10 – Time evolution of critical current in Nb_3Sn conductors.

This study was made on 3 Sectors samples with a diameter of 0.820 mm and demonstrates a current peak around 130–150 h of tin diffusion; similar analysis on High Field wires of the same diameter and 3 Sectors wires with larger diameter (0.835 mm) have recently revealed the same peak shifted at nearly 180 h. This is explainable with the hypothesis that in High Field configuration the absence of the three channels retards tin diffusion toward peripheral filaments while in the latter case the increase of wire diameter implies an analogous time extension due to greater surface.

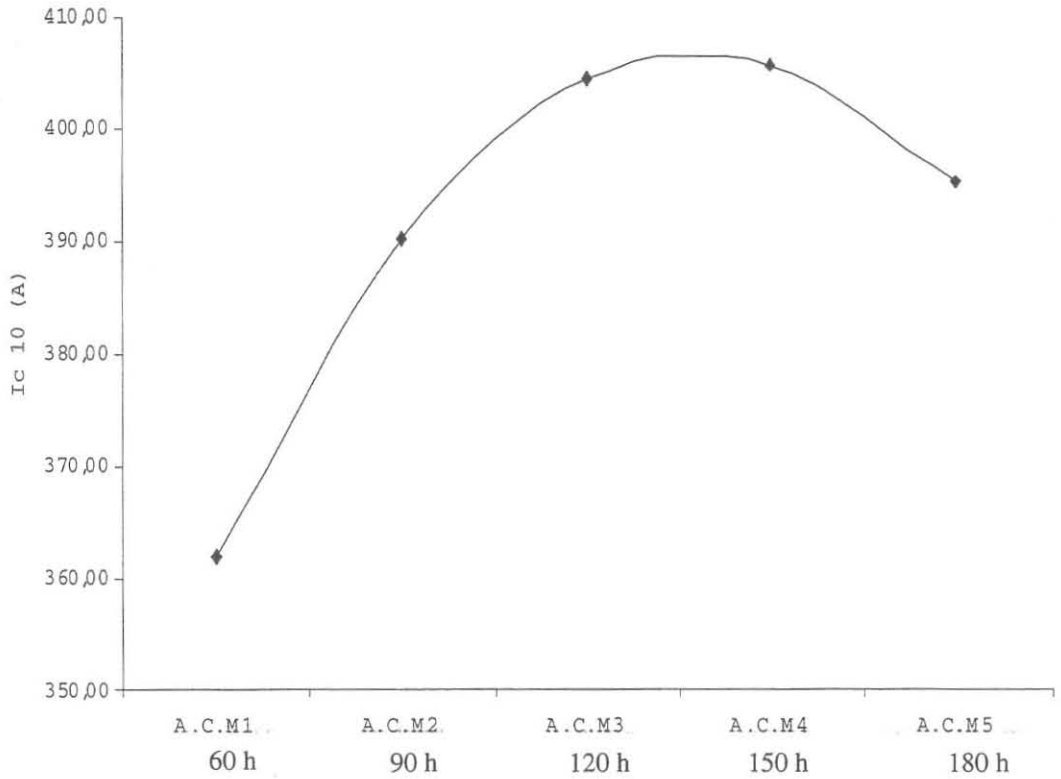

FIG. 11 – Measured critical current in samples with different thermal treatment (*EM–3sect–95–virgin*).

4.3 I_C DEGRADATION DUE TO CABLING AND CU RRR

Measurements on virgin strands are not always representative of the quality of a conductor since for normal apparatus multi-wire cables are used and the process of assembling these ones often implies a certain degree of lowering of current throughput; analysis of transport properties on wires extracted from cables are then necessary. We must nevertheless consider that the straightening of the kinks involves a further degradation, which we cannot avoid, unless making measurements on the whole cable.

As can be seen in figure 12 and in table 2, degradations are always limited to a maximum of about 18%, even less in the cable which wasn't cabled by Europa Metalli but was processed at the Lawrence Berkeley Laboratory (3) in the context of a collaboration between our labs (about 10%). A similar degradation is visible for n values, due to sausaging of strands in the kinks.

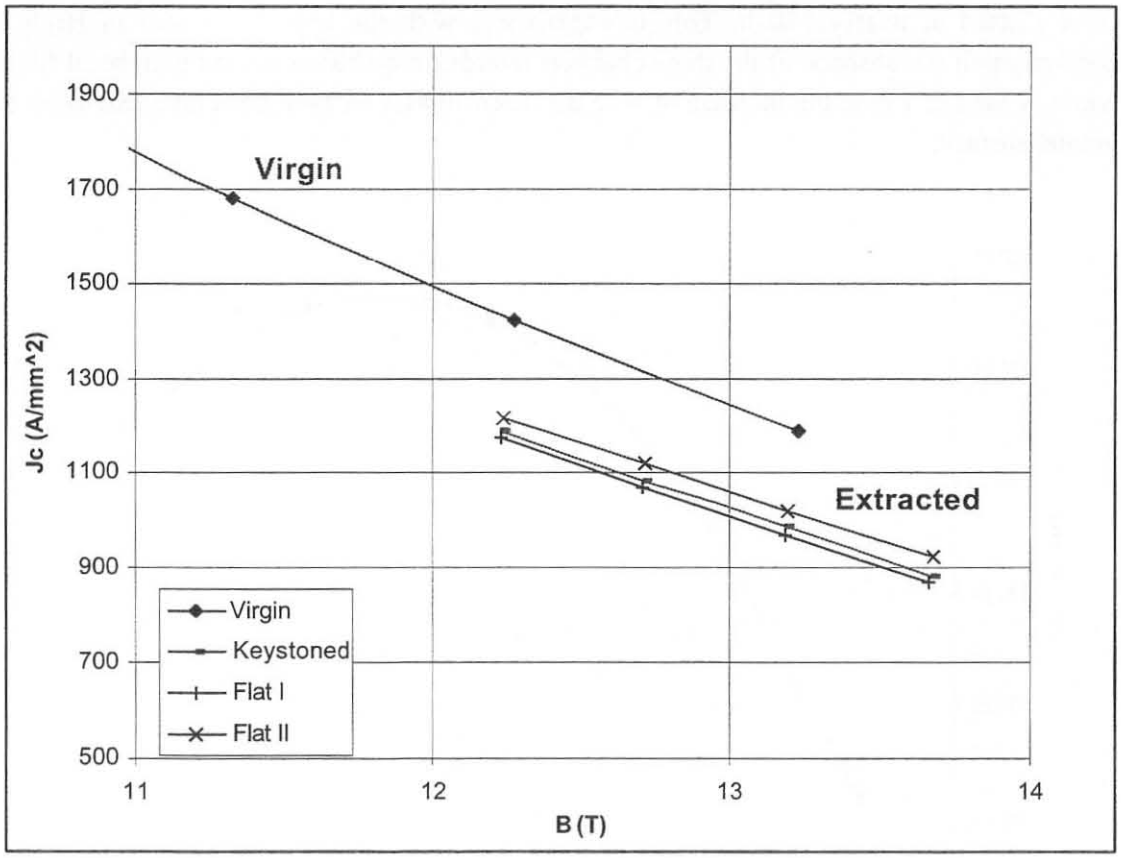

FIG. 12 – J_c degradation with cabling in 3 Sectors–'95 wire.

RRR value (copper residual resistivity ratio) was also measured for extracted cable between 0 °C and 20 K, resulting about 70, which is not very satisfactory for a conductor treated at high

temperatures for weeks and indicates a possible small diffusion of tin through the barriers. Values larger than 50-60 are nevertheless sufficient for accelerator magnets.

TABLE 2 - J_c degradation due to cabling. (# made at LBL)

Type of cabling (3 sectors)	Strands (No.xϕ)	Width (mm)	Thickness (mm)	Filling factor	I_c degradation (12-14 T)
Flat I	36 x 0.820	15.0	1.48	87 %	18-19%
Flat II	36 x 0.820	15.0	1.48	87 %	14-15%
Keystoned 1°	36 x 0.820	15.0	1.48	87 %	17%
Keystoned 1.2° #	36 x 0.835	15.1	1.53	85 %	10-11%

4.4 I_C DEGRADATION VS TRANSVERSE STRESS

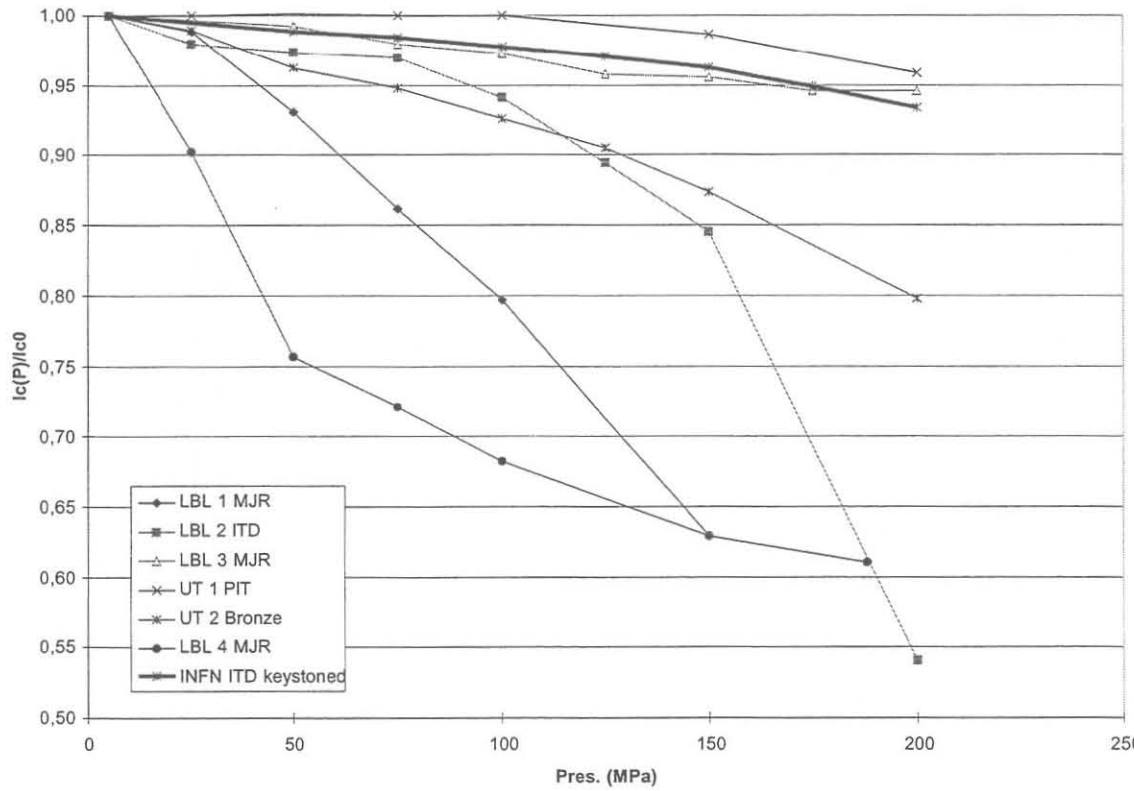

FIG. 13 – I_c degradation versus applied transverse stress in 3 Sectors Keystoned cable compared with other Nb_3 Sn conductors.

[MJR = Modified Jelly Roll; ITD = Internal Tin Diffusion; PIT = Powder In Tube]

The typical transverse pressure acting on the winding of a quadrupole is in the range of 150 MPa. To account for the behavior of critical current when applying such a stress, two cables were sent to the University of Twente where a special facility, capable of measuring cable I_c under transverse pressure, is available. One sample was of flat cable and the other from the 1° keystoned cable.

The critical current of the cables at (almost) zero pressure and 11 T was first measured, followed by the same measurements in different applied pressure conditions. Results [4] for the keystoned cable are shown in figure 13. As can be seen, the degradation of critical current in our cable, as compared with other similar ones from different producers, was very limited, less than 7% at 200 MPa and only 1% irreversible.

The moderate sensitivity of this conductor to stress, already shown by the moderate cabling degradation, is one of the most important characteristics of this conductor. We think that the multi-bundle arrangement with individual barrier around each filament bundle and the very careful heat treatment schedule, that helps to avoid holes and cavities inside the wire (which are always stress concentration points), are the reasons for this very good behavior. Micrographs of the cross section of reacted wires confirms that there are no cavities or voids in the central core where tin is positioned (see previous figures).

5. EFFECTIVE FILAMENT SIZE

For accelerator magnet applications a low magnetization of the superconductor is generally required in order to reduce field distortions and AC losses. For this reason and according to the stability conditions on flux jumping, little effective filament sizes are generally needed for a superconductor.

Adiabatic stability imposes a fine subdivision of the superconducting element (for Nb_3Sn, 300 μm has been computed as maximum tolerable size) but field uniformity puts more severe limits, in the order of 10 –20 μm. This is in contradiction with the demand of high critical current values, generally obtained with layouts that possess very large filament size.

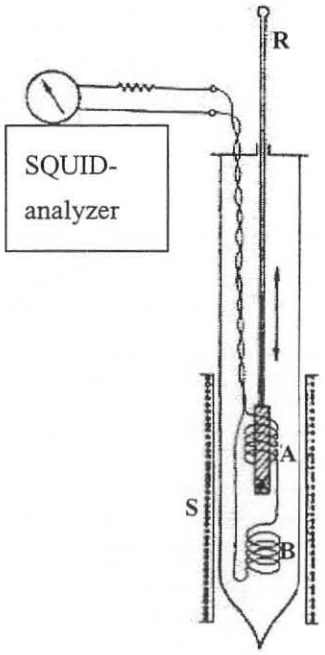

FIG. 14 – Schematic representation of the apparatus for magnetic measurements.

The effective filament size was deduced by measuring, at CISE laboratory in Milan, a full magnetization cycle from –5 T to +5 T with a SQUID based apparatus in which the sample (a 6 mm Ø, 5 mm high spiral) is moved inside and outside of an analysis coil in an applied magnetic field at liquid helium temperature.

The schematic structure of this apparatus is shown in figure 14; the sample is moved upward and downward inside the two coils, A and B (connected in series opposition to cancel parasitic effects), with a background field produced by the solenoid S. The flux variations of the two coils are registered by a SQUID based analyzer, by which a direct measure of sample magnetization is extracted.

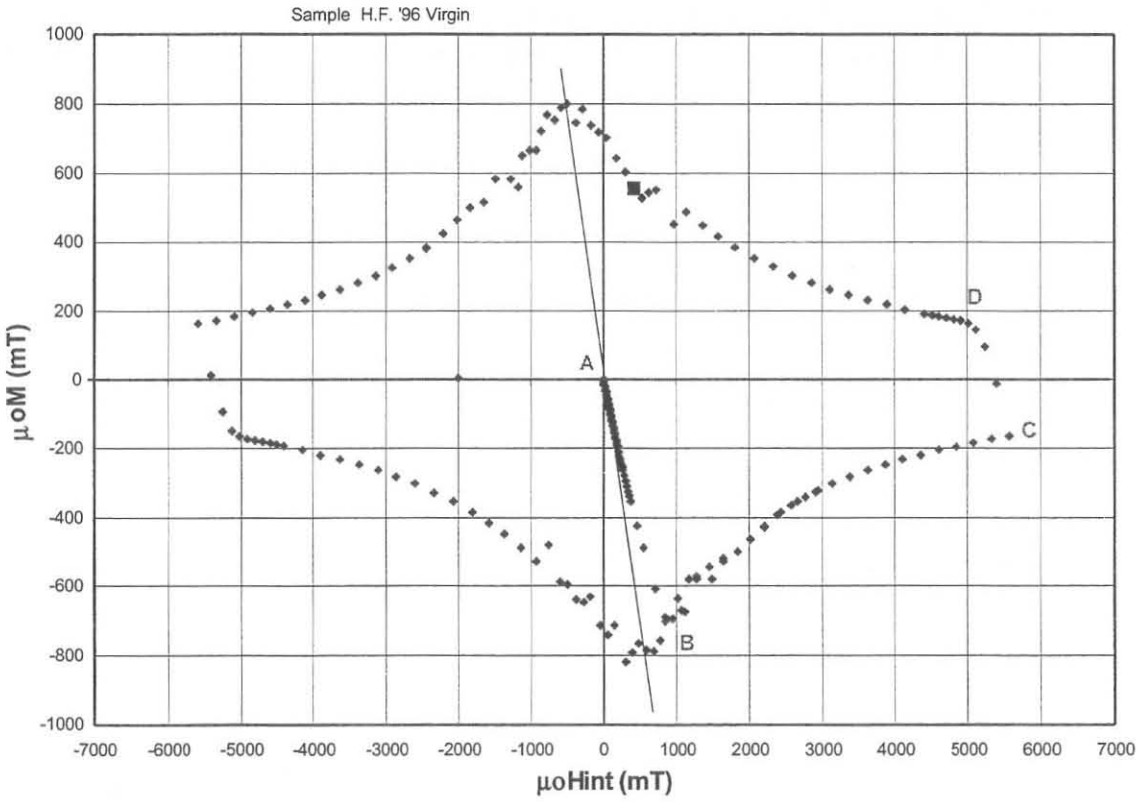

FIG. 15 – Example of magnetization cycle for effective filament size determination: AB represents perfect Meissner behavior, besides which field penetrates; from the width of CD effective filament size is deduced.

According to the "critical state model" (5), the effective filament size is proportional to sample magnetization and can therefore be derived by this with simple algebraic calculations.

The values obtained in 3–Sectors layout wires are very high, as supposed: nearly 60 μm in virgin strands and 80 μm in extracted ones. For High Field configuration the results are even worst: a little more than 100 μm. This high value is approximately equal to the size of the barrier, which indicates that the island behaves as a single bigfilament; besides, tunneling between filaments contribute to this effect. Solutions to the problem could be found in the use of more resistive bronze by nickel doping (to limit tunneling), the fragmentation of the barrier together with the use of different materials and the finer subdivision of the wire by increasing the number of bundles. These should preserve high J_c but lower effective filament size.

By the analysis of the characteristic χ–T (magnetic susceptibility Vs temperature) the important information about critical temperature of our superconductors was also derived, which is about 17–17.5 K in all samples. Besides we could deduce the percentage of non-reacted Nb as represented by the skip of experimental points near Nb transition temperature (see fig. 16).

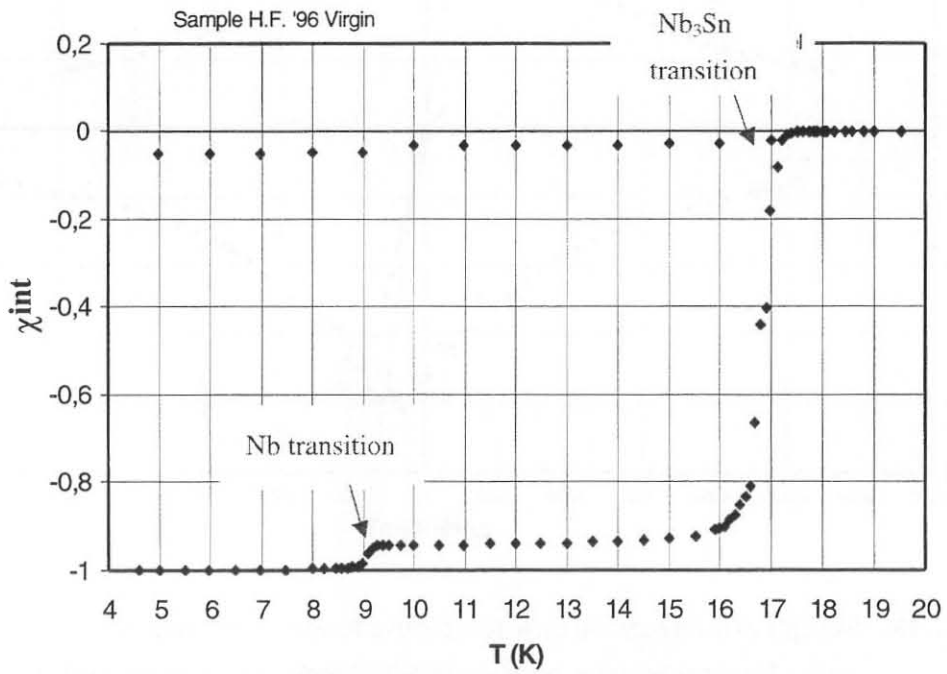

FIG. 16 – Example of transition temperature in High Field sample as deduced from χ versus T diagram.

Complete series of effective filament sizes is reported in summary table 3.

TABLE 3 – Summary of all measurements (J_c values are self–field corrected).

IDENTIFICATION	ϕ (mm)	α	B range 4.2K	B range 2.2K	J_{c10} (B//–12 T - 4.2K) (A/mm^2)	n (B//-12 T)	ϕ_{eff} (5T) (μm)	Notes
EM–3sect–95–virgin–1	0.820	1.1	5÷13	8÷14	1492	41	57	
EM–3sect–95–virgin–3	0.820	1.1	10÷13.5	9÷13	1445	28	–	
EM–3sect–95–cabl.key.–1	0.820	1.1	12÷13.5	–	1248	21	82	Rutherford cable Keystoned–36 strands
EM–3sect–95–cabl.flatI–1	0.820	1.1	12÷13.5	–	1241	23	80	Rutherford cable Flat I –36 strands
EM–3sect–95–cabl.flatII–1	0.820	1.1	12÷13.5	–	1299	24	71	Rutherford cable Flat II –36 strands
EM–High Field–96–virgin–1	0.820	1.1	5÷13	–	1492	21	114	
EM–High Field–96–virgin–2	0.820	1.1	–	–	–	–	–	RRR=70 at 24 °C
EM–High Field–96–virgin–3	0.820	1.1	4÷13	10÷14	1363	18	–	
EM–3sect–96–virgin–1	0.835	1.1	12÷13.5	–	1481	37	71	
EM–3sect–96–LBL601A	0.835	1.1	12÷13.5	–	1357	22	76	Rutherford cabling made at LBL
VAC–Ta–I–HP–96–Ar–1	0.8	0.211	12÷13.5	–	591 (B anti//)	55	33	Internal stabilization B anti// only
VAC–Ta–I–HP–96–vac–2	0.8	0.211	12.5÷13.5	–	–	–	35	Internal stabilization
VAC–Ta–I–HP–96–vac–3	0.8	0.211	7÷13.5	–	703	46	–	Internal stabilization
EMDSC–smpl–0002–98–1	0.90	1.1	11.5÷13	–	1981	26	–	High Field evolution
EMDSC–smpl–0002–98–2	0.90	1.1	12÷13.5	–	1996	30	–	High Field evolution
EM–0023–NbSn–AC–98–1	0.90	1.11	9÷13.5	13÷14	1975	47	108	High Field evolution RRR=32 at 24 °C
EM–A.C.M.–1	0.9	1.12	12÷13.5	–	1277	19	–	T.T.: 650°C x 60 h
EM–A.C.M.–2	0.9	1.14	10÷13.5	–	1393	22	–	T.T.: 650°C x 90 h
EM–A.C.M.–3	0.9	1.13	12÷13.5	–	1428	23	–	T.T.: 650°C x 120 h
EM–A.C.M.–4 bis	0.9	1.11	9÷13.5	–	1333	20	–	T.T.: 650°C x 150 h
EM–A.C.M.–5	0.9	1.12	12÷13.5	–	1384	21	–	T.T.: 650°C x 180 h
EM–CRIS A up	0.9	1.1	11.5÷13.5	–	1558	32	–	Thermal treatment made by CRIS
EM–CRIS B up	0.9	1.1	11÷13.5	–	1589	34	–	Thermal treatment made by CRIS
EM–CRIS C up	0.9	1.1	12.5÷13.5	–	–	–	–	Thermal treatment made by CRIS
EM-CRIS A down	0.9	1.1	–	–	–	–	–	Under 150 A
EM–CRIS B down	0.9	1.1	11.5÷13.5	–	1258	15	–	Thermal treatment made by CRIS

6. SCALING LAWS

The most important work on "Scaling laws for flux pinning in hard superconductors" was elaborated by Kramer in 1973 (6) and predicts a law of the kind $B^{-1/2}\cdot(1-b)^2$ for J_c.

More recent works (7) estimated the dependency of critical current density by reduced temperature; combining these different theories, together with the addiction of a phenomenological term containing reduced field as made by Summers (8), a more precise formulation on J_c behavior has been proposed, which is just as follows:

$$J_c(B,T) = \underbrace{C\cdot(1-t^2)^2}_{\text{temperature corr.}}\cdot\underbrace{b^{-1/2}}_{\text{Summers corr.}}\cdot\underbrace{B^{-1/2}\cdot(1-b)^2}_{\text{Kramer}}$$

It is well known that Nb_3Sn and all A15 compounds in general have a strong dependence on deformation, degrading the critical current at even small values of mechanical strain, ε; at 12 T, a strain as little as 0.2% can produce a decrease in critical current density equal to approximately 10%, which is not negligible considering that superconducting apparatus are commonly studied to work at their maximum limit.

Expressing dependence by ε (9) of all terms in previous expression a complete formulation of J_c versus magnetic field, temperature and strain there results:

$$J_c(B,T,\varepsilon) = C(\varepsilon)\left(B^*_{c2}(T,\varepsilon)\right)^{-1/2}\left(1-t^2\right)^2 b^{-1/2}(1-b)^2 \ ,$$

where

$$B^*_{c2}(T,\varepsilon) = B^*_{c20}(\varepsilon)\left(1-t^2\right)\left[1-0.31t^2(1-1.77\ln t)\right] \ ,$$

$$t = T/T^*_c(\varepsilon) \ ,$$

$$b = B/B^*_{c2}(T,\varepsilon) \ ,$$

$$C(\varepsilon) = C_0\left(1-a|\varepsilon|^u\right)^{1/w} \ .$$

We must remind that the composite nature of Nb_3Sn implies that reacted material is originally in a pre-compressive status, given by the differential thermal contractions of the elements composing the superconductor/bronze system; using the right thermal dilation coefficients it can be shown that the pre–compressive strain is nearly equal to 0.3%.

Expressing the strain as the sum of the pre-compressive strain and the electromagnetic one, due to electromagnetic forces acting on the superconductor when it is carrying current, we may thus make a fit of the experimental values with the theoretical form obtained. The varying parameters of our fit are a,u,w,C_0, B^*_{c2m} e T^*_{cm}. It was also found that values are better fitted by the expression above when the exponent of the Summer correction is–3/4 rather than –1/2.

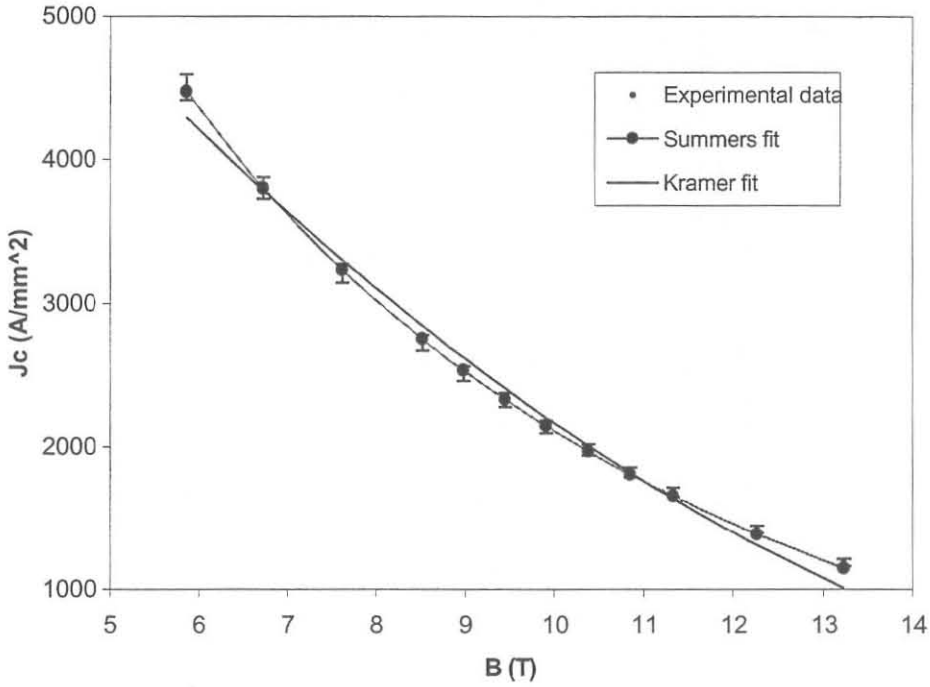

FIG. 17 – Comparison between the two models.

It is clear that the importance in deriving good scaling laws for the superconductor resides in the fact that for each application the precise knowledge of the limits of use of the material are required, and it's so necessary to derive its *critical surface* or at least its isotherms. Global critical surfaces for Nb_3Sn are not easily found in literature (critical surfaces of NbTi are usually known, for this material is well known and its properties more easy to measure); the use of the model elaborated allows to represent the critical surface of this brittle material, as shown in figure 18 with some isotherms also displayed.

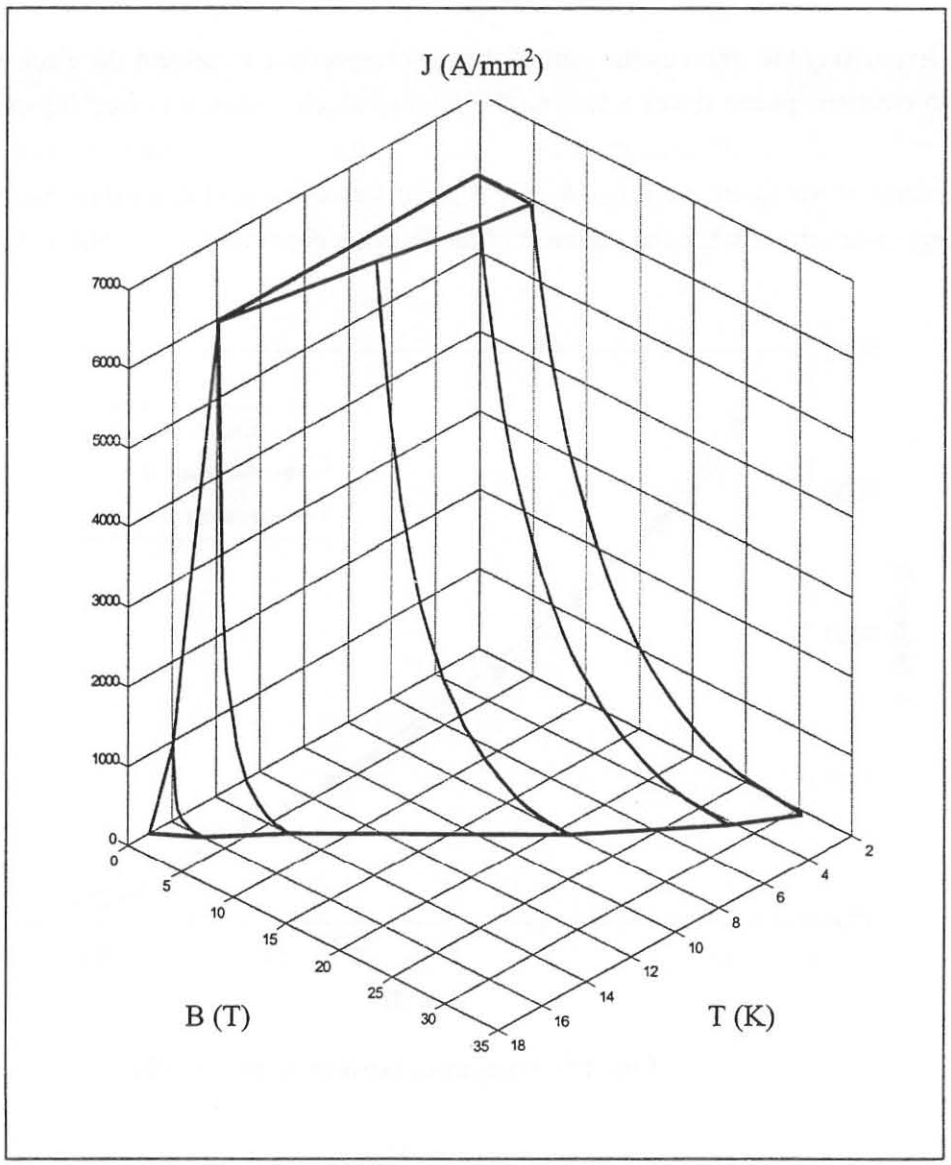

FIG. 18 – Critical surface for Nb_3Sn.

7. Ø 0.9 MM, HIGH FIELD WIRE

On our request Europa Metalli has recently manufactured a superconducting wire in the High Field layout with a diameter little greater than the previous ones, that is 0.9 mm. This was done with the aim of verifying the possibility of obtaining greater current densities increasing cross section for tin diffusion and for testing doping of the barrier with 1% Ti.

Record values of critical current densities have been obtained in this new wires, though at the expenses of a good stability of the wire. In fact, measurements on these samples have been

always disturbed by premature quenching, probably not due to movements (the last sample was embedded with a bi-component resin, which guarantees great rigiditybut prevents a good thermal

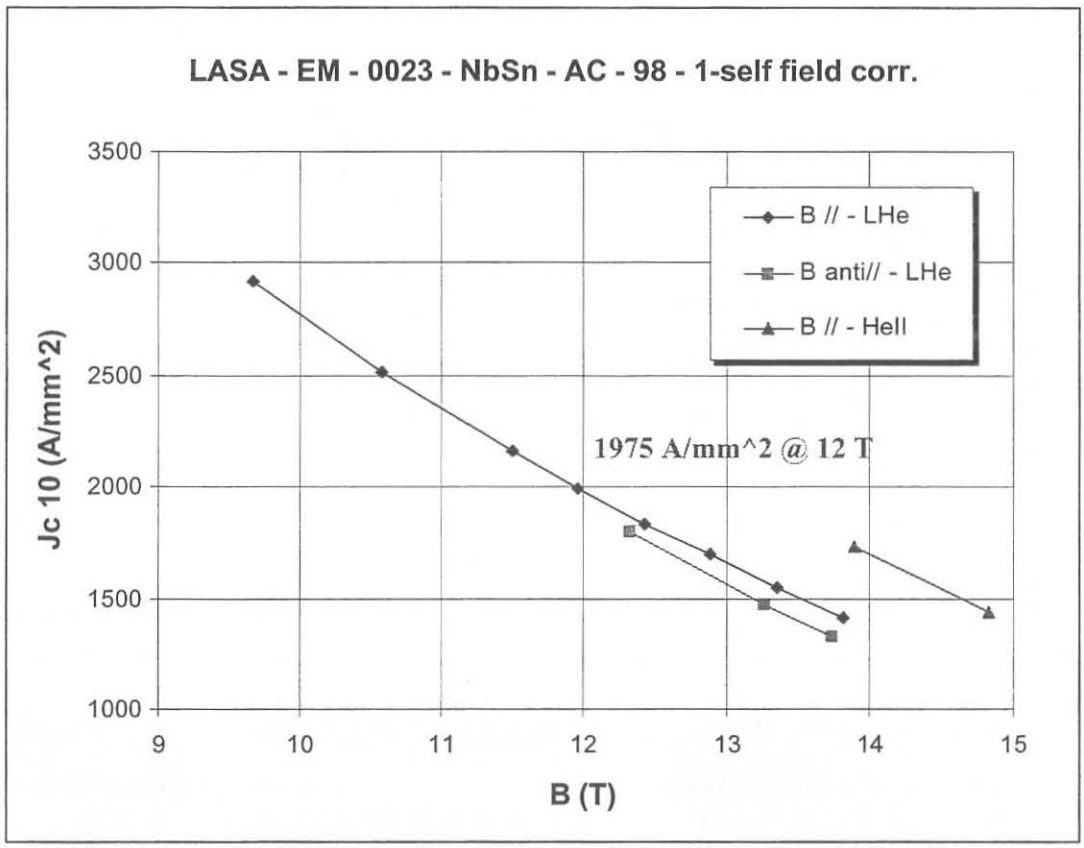

FIG. 19 – Experimental results for the new High Field wire.

exchange) but deriving from intrinsic instability of the wires (see also n-B plot). As can be seen in figure 19, which represents the best results obtained ("best" is referred to the largest number of experimental points not to the highest J_c values, that are almost the same in all samples up to now measured), not all measurements in both field polarizations were possible and only two measures at 2.2 K in parallel field. We hoped to have some answers to this anomalous behavior from the magnetic analysis of wires but effective filaments sizes are just as those of the previous samples (108 μm at 5 T) and so well below the stability limit for Nb_3 Sn, which is nearly 300 μm. More helpful are the microphotographs which show too close filaments in wires not yet reacted. Maybe less copper between bundles or tin contaminate copper, as possibly shown by a small value of RRR (which was measured on a sample resulting as small as 32), are at the basis of this loss of stability. Future studies could account for this strange behavior.

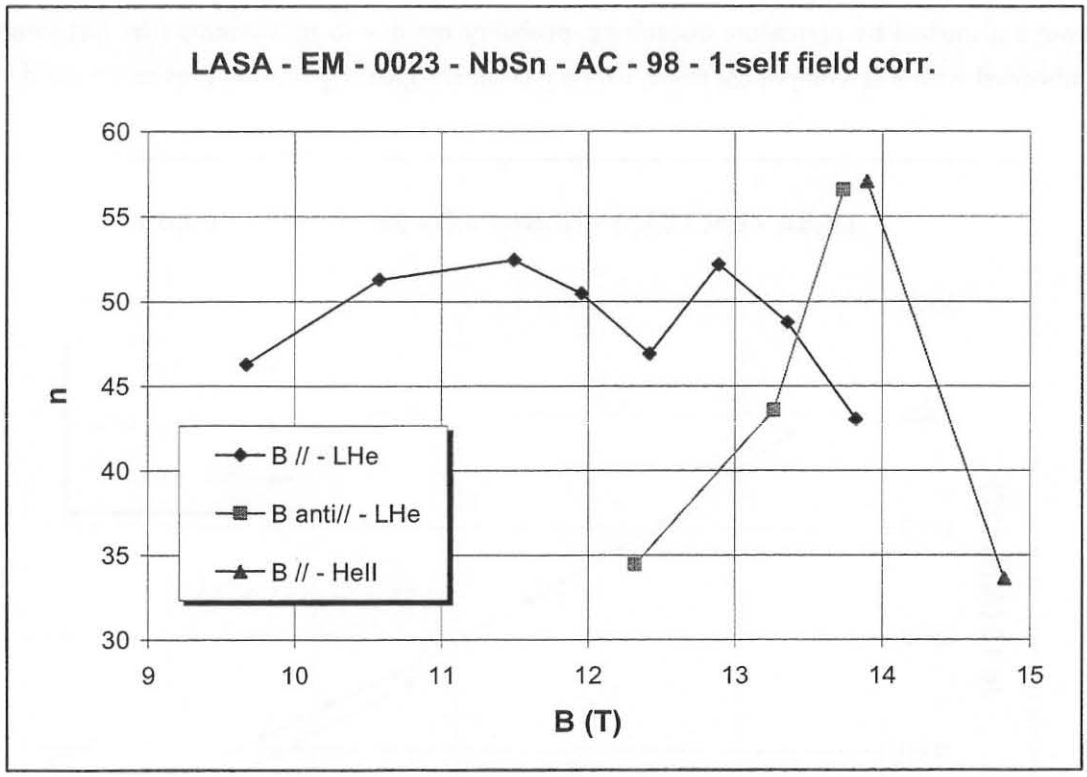

FIG. 20 – n versus B plot for 0.9 mm High Field wire (behavior is notregular due to its instability).

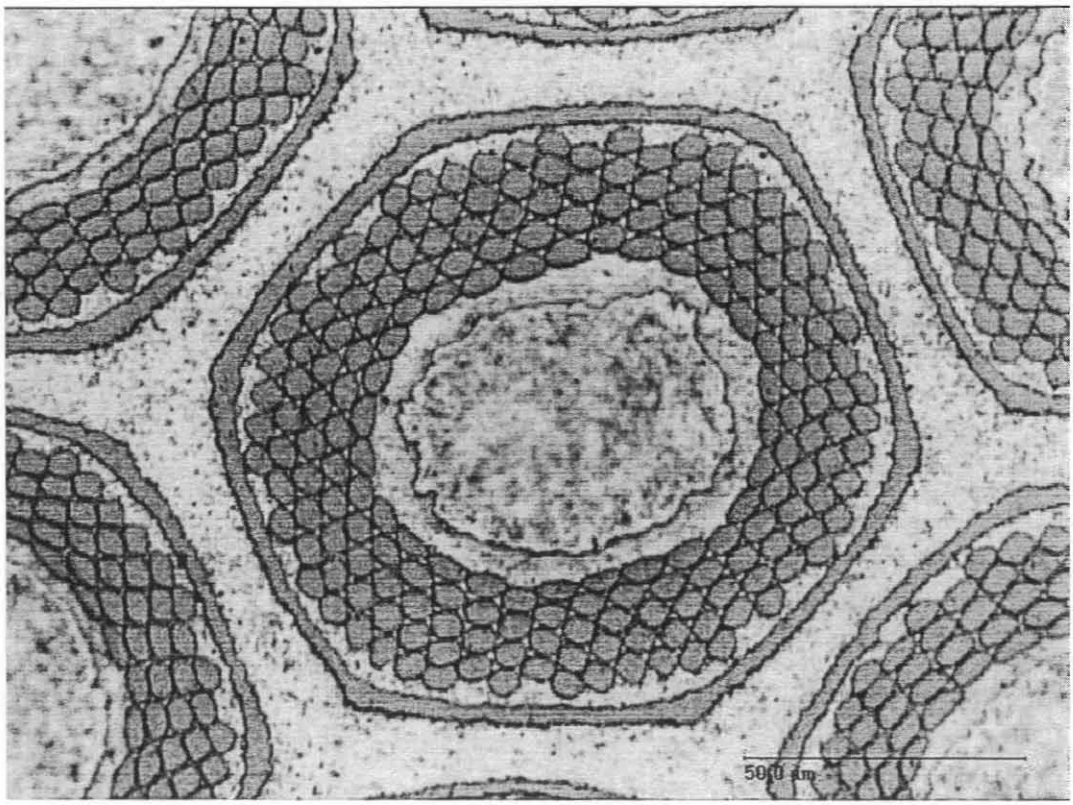

FIG. 21 – Detail of a 0.9 mm High Field wire section. Note the bridging between filaments.

8. CONCLUSIONS

High critical current density values are a good promise for the feasibility of a Nb_3Sn quadrupole, being satisfied the work condition of 1800 A/mm^2 at 12 T. I_c degradation in terms of cabling and transversal stresses have been found to be low and RRR values are satisfactory. Due to these good results, a prototype winding in a race-track form with a length of 400 mm and double layer has recently been realized with a 3 Sectors, flat Rutherford cable and will be soon tested at LASA.

Effective filament sizes are nevertheless too high, though a possible way of limiting these has been here proposed (more resistive bronze and smaller bundle size); future studies could also explain the instability in High Field wires of the last generation, first of all other RRR measurements to deduce the goodness of copper, maybe contaminate by tin diffusion.

ACKNOWLEDGEMENTS

The authors fully acknowledge the support and cooperation of Europa Metalli in providing the conductors and Mr. Ottoni of CISE (now ENEL Ricerche) for his measurements.

REFERENCES

(1) "The Large Hadron Collider" – conceptual design, CERN/AC (1995)

(2) G. Ambrosio, G. Bellomo, F. Broggi, L. Rossi, "Design of a Nb_3Sn high gradient low-beta quadrupole magnet", MT-15 (1997)

(3) Ron Scanlan, LBNL, USA, private communication

(4) H. Boschmann et al., "The effect of Transverse Loads up to 300 MPa on the Critical Currents of Nb_3Sn Cables, *IEEE Trans. On Mag.* Vol 27, p. 1831, March 1991

(5) C. P. Bean, *Rev. Of Mod. Phys.*, Vol. 36, p. 31 (1964)

(6) E. J. Kramer, "Scaling Laws for Flux Pinning in Hard Superconductors", *J. of Appl. Phys.*, Vol.44, No.3 (March 1973)

(7) W. A. Fietz and W. W. Webb, *Phys.Rev.*, 178, 657 (1969)

(8) L. T. Summers, M. W. Guinan, J. R. Miller and P. A. Hahn, "A model for the prediction of Nb_3Sn critical current as a function of field, temperature , strain and radiation damege", Lawrence Livermore National Laboratory (1990)

(9) J. W. Ekin, F. R. Pickett and A. F. Clark, *Proc. Int. Cryo. Mat. Conf.* (aug. 1975), *Adv. Cryo. Eng.* (1977)